



Cite this: DOI: 10.1039/c4nj01695e

Substituted triphenylamines as building blocks for star shaped organic electronic materials†

Daniel Lumpi,[‡] Brigitte Holzer,[‡] Johannes Binting,^{ab} Ernst Horkel,^{*a} Simon Waid,^c Heinz D. Wanzenböck,^c Martina Marchetti-Deschmann,^d Christian Hametner,^a Emmerich Bertagnoli,^c Ioannis Kymissis^b and Johannes Fröhlich^a

A versatile synthetic protocol toward a series of various substituted triphenylamine derivatives serving as building blocks for organic electronic materials was developed. Key steps during synthesis were either Ullmann condensations or nucleophilic aromatic substitutions giving rise to structural modification of triphenylamines and their electronic nature. In turn, these scaffolds were exemplarily attached to a dendritic tris(2-thienyl)benzene core affording star shaped organic semiconducting materials which were characterized regarding their photo-physical, electro-chemical and thermal properties. A strong influence of the substituent's nature on both photo-physical and morphological thin film characteristic of star shaped target compounds was observed. The applicability of these materials in organic electronic devices was demonstrated in an organic field effect transistor configuration yielding a hole mobility of nearly $10^{-3} \text{ cm}^2 \text{ V}^{-1} \text{ s}^{-1}$. The performance of the materials can be correlated to the substituents applied.

Received (in Montpellier, France)
30th September 2014,
Accepted 15th December 2014

DOI: 10.1039/c4nj01695e

www.rsc.org/njc

Introduction

Organic electronic (OE) thin film devices have gained raising interest from academia and industry due to the variety of possible applications with enormous commercial potential.¹ This field covers the application of conducting and semi-conducting organic materials within electronic devices such as organic field effect transistors (OFETs),² organic light emitting devices (OLEDs)³ and organic photovoltaics (OPVs).^{4,5} The application of these materials in the field of organic electronics allows for solution processability, thus rendering OE-technology compatible with established high-throughput printing techniques and with the potential to realize thin, flexible and light-weight devices with low manufacturing costs.⁶

In general, a high charge carrier mobility is mandatory for the performance of different devices and strongly depends both

on the molecular structure and the morphology of the semiconducting material.^{2,7} Therefore, a broadly applicable material with high charge carrier mobility independent of processing techniques is desirable.^{8,9} The quest for novel compounds is an ongoing process in material science.

Poly- and oligothiophene based compounds have a long history in the field of OE.¹⁰ While high hole mobilities (up to $1.3 \text{ cm}^2 \text{ V}^{-1} \text{ s}^{-1}$) have been observed for thin films of poly-(3-hexylthiophene) (P3HT),¹¹ the material cannot be used in the light emitting layers of an OLED due to fluorescent self-quenching caused by strong π - π stacking.¹² Another useful class of OE materials are modified triphenylamine (TPA) structures, which have excellent electron donor and hole transport properties.¹³⁻¹⁷ The combination of these structural scaffolds results in a material class incorporating good charge carrier transport as a result of the oligothiophene unit and enhanced luminescent properties by circumventing self-quenching (e.g. **BMA-1T**, Fig. 1).¹⁸ Moreover, star-shaped compounds are found to exhibit better solubility and film-forming properties than their linear counterparts.^{8,19,20}

Combining TPA and thiophenes in C_3 symmetric configurations leads to enhanced electronic and luminescent properties with the benefit of solution processability.²¹ To realize C_3 symmetry, one can think of two possible molecular designs. One possibility is to use the TPA moiety as a central node with thiophene moieties as dendrons.^{19,22,23} Alternatively, a core (e.g. tris(2-thienyl)benzene) can be used to ensure C_3 symmetry bearing TPA units as side arms.²⁴ Based on these two possible

^a Institute of Applied Synthetic Chemistry, Vienna University of Technology, Getreidemarkt 9/163OC, A-1060 Vienna, Austria.

E-mail: ernst.horkel@tuwien.ac.at

^b Department of Electrical Engineering, Columbia University, 520W 120th street, Suite 1300, 10027 New York, NY, USA

^c Institute of Solid State Electronics, Vienna University of Technology, Floragasse 7, A-1040 Vienna, Austria

^d Institute of Chemical Technologies and Analytics, Vienna University of Technology, Getreidemarkt 9/164IAC, A-1060 Vienna, Austria

† Electronic supplementary information (ESI) available: ¹H and ¹³C NMR spectra of compounds **6c**, **6e-1**, **8c**, **8e-g**, **2**, **S2-3**, absorption and emission spectra of compounds **S1-3** and HOMO-LUMO plots of **S1-3**. See DOI: 10.1039/c4nj01695e
‡ Daniel Lumpi and Brigitte Holzer contributed equally to this article.

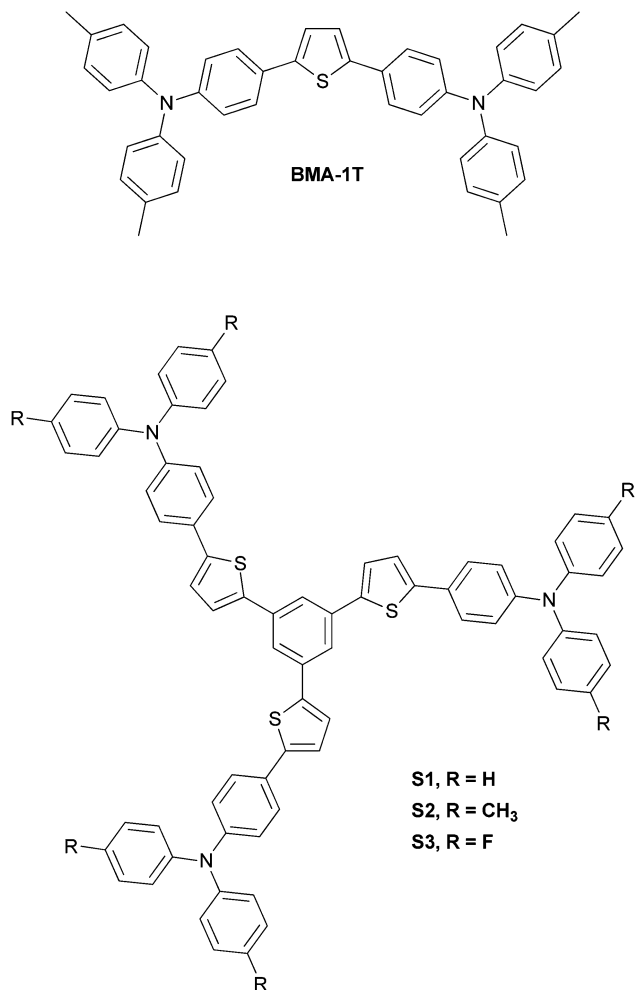


Fig. 1 Linear motifs (top) presented by Noda,¹⁸ star shaped molecules described in this work (bottom).

structural connectivities, this paper focuses on the latter possibility, since substituent alteration on the three TPA moieties constituting the outer sphere of the molecule strongly influences glass- and film-forming behaviour⁸ of the resulting materials, in turn affecting device performance.

Due to the widespread application of TPA-based compounds as building blocks in the field of organic electronics,²⁵ the synthetic protocol presented in this work is of considerable interest for the molecular design and potential modifications (*e.g.* in terms of photo-physical properties) toward a broad range of novel materials. Fine tuning of material properties can be realized by applying structurally and electronically diverse TPA motifs. However, due to the broad spectrum of substituents (electron donating or withdrawing) attached to the TPA, no general synthetic protocol is available. Access to TPAs bearing electron donating substituents is often described in literature, mainly applying Ullmann condensation.²⁶ On the other hand, this synthetic technique often fails when applied towards the synthesis of electron withdrawing groups. As a result of our investigations to overcome this drawback, we present a general protocol using nucleophilic aromatic substitution in order to

gain access to TPAs bearing electron withdrawing substituents. Reaction conditions for the consecutive transformation to the above-mentioned boronic acid esters also depend on the substituents' nature. While lithiation protocols can be applied for most TPAs under investigation, Miyaura borylation is required for TPAs bearing $-M$ substituents (Scheme 2).

With these TPA boronic acid esters in hand, a set of three star shaped compounds **S1–3** was realized using a Suzuki reaction. This nontoxic procedure proved superior in yield to a previously reported procedure incorporating a Stille reaction for the same compound **S1**.²⁴

Measurements of electro-chemical and optical properties (*e.g.* fluorescence spectra and quantum yields) of the star shaped compounds **S1–3** reveal the strong influence of the substituents' nature on the TPA moiety on the above-mentioned properties. The materials were characterized with respect to thermal stability, film-forming upon spin coating and semiconducting behaviour (charge carrier mobility in OFET configuration) to probe device applicability. Mobilities of almost $10^{-3} \text{ cm}^2 \text{ V}^{-1} \text{ s}^{-1}$ and low threshold voltages of approx. 0 V were recorded using methyl-TPA substituted derivative **S2**.

Experimental section

Synthesis and characterization

Substances purchased from commercial sources were used as received. Anhydrous *N,N*-dimethylformamide (DMF), *n*-butyllithium solution (2.5 M in hexanes) and 1,3,5-tribromobenzene were purchased from Aldrich Chemical Co. Isopropyl pinacol borate²⁷ (CAS 61676-62-8), (IPr)Pd(allyl)Cl²⁸ (CAS 478980-03-9) were synthesized according to literature. Anhydrous tetrahydrofuran (THF), diethyl ether, toluene were prepared immediately prior to use by a PURESOLV-plant (*it-innovative technology inc.*). Technical grade solvents were distilled prior to use. Analytical TLC was performed on Merck silica gel 60 F254 plates. Chromatographic separations at preparative scale were carried out on silica gel (Merck silica gel 60, 40–63 μm), alox or RP-gel. Nuclear magnetic resonance (NMR) spectra were obtained using a Bruker DPX-200 or Avance DRX-400 Fourier transform spectrometer operating at the following frequencies: DPX-200: 200.1 MHz (¹H) and 50.3 MHz (¹³C); DRX-400: 400.1 MHz (¹H) and 100.6 MHz (¹³C). The chemical shifts are reported in delta (δ) units, parts per million (ppm) downfield from tetramethylsilane using solvent residual signals for calibration. Coupling constants are reported in Hertz; multiplicity of signals is indicated by using following abbreviations: s = singlet, d = doublet, t = triplet, q = quartet. The multiplicity of ¹³C signals were obtained by measuring JMOD spectra. UV/VIS absorption and fluorescence emission spectra were recorded in THF solutions ($1 \mu\text{g mL}^{-1}$) with a Perkin Elmer Lambda 750 spectrometer and an Edinburgh FLS920, respectively. Cyclic voltammetry was performed using a three electrode configuration consisting of a Pt working electrode, a Pt counter electrode and an Ag/AgCl reference electrode and a PGSTAT128N, ADC164, DAC164, external, DI048 potentiostat provided by Metrohm Autolab B. V. Measurements were carried

out in a 0.5 mM solution in anhydrous DCM (oxidation scan) with Bu_4NBF_4 (0.1 M) as the supporting electrolyte. The solutions were purged with nitrogen for 15 minutes prior to measurement. HOMO energy levels were calculated from the onset of oxidation. The onset potential was determined by the intersection of two tangents drawn at the background and the rising of oxidation peaks. High-resolution mass spectra (HRMS) were acquired as radical cations using a SYNAPT HDMS instrument (Waters, Manchester, UK) equipped with a matrix-assisted laser desorption/ionization (MALDI) source (MALDI-HRMS). Samples were applied at 1 mg mL^{-1} in THF on stainless steel using nitroanthracene (3 mg mL^{-1} in THF) as MALDI matrix. All MS spectra were recorded as accurate mass data with Angiotensin II (m/z 1046.542) as internal lock mass achieving a mass accuracy of 15–40 ppm (*i.e.* $\Delta m/z$ 0.01–0.04 amu). GC-MS measurements were conducted on a GC-MS hyphenation from Thermo Finnigan: focus GC with a BGB5 column ($l = 30 \text{ m}$, $\varnothing = 0.25 \text{ mm}$, $0.25 \mu\text{m}$ film); DSQ II Quadrupole (EI^+ mode). The thermal behavior of substances **S1–3** was studied with differential scanning calorimetry (DSC) and thermogravimetric analysis (TGA) using a Netzsch simultaneous thermal analyzer (STA 449 F1 Jupiter). Powder samples with a mass of approx. 10 mg were lightly pressed into the bottom of open aluminum pans and heated at $10 \text{ }^\circ\text{C min}^{-1}$ from $25 \text{ }^\circ\text{C}$ to $500 \text{ }^\circ\text{C}$ under N_2 gas at a flow rate of 40 mL min^{-1} . The STA 449 type-K thermocouples were calibrated using indium, tin, bismuth and zinc metals.

Bottom-gate, top-contact OFETs were fabricated on ITO substrates with a 250 nm layer of vacuum deposited parylene-C which serves as a common gate electrode/gate dielectric structure. The substrates were ultrasonically cleaned with water, acetone and isopropanol followed by a 20 min treatment of UV/ozone. Compounds **S1–3** (25 nm) were vacuum deposited through a shadow mask ($p = 10^{-7}$ Torr, rate 0.1 \AA s^{-1}). The devices were completed by evaporation of gold source and drain electrodes (50 nm) on top. All characterizations were performed in ambient air. Current–voltage characteristics of the fabricated devices were recorded using a Keithley model 4200 semiconductor characterization system. Output and transfer characterization were recorded for at least four samples of the same channel width ($W = 2000 \mu\text{m}$) and channel length ($L = 100 \mu\text{m}$).

The spin-coated samples were prepared by the following procedure: the ITO substrates were ultrasonically cleaned with water, acetone and isopropanol followed by blow-drying with N_2 . 400 μL of a solution of the organic substance in chloroform (20 mg mL^{-1}) was prepared and filtered through a syringe filter (Teflon \varnothing 25 mm, $0.20 \mu\text{m}$). Consecutively 300 μL of the prepared organic solution was spin-coated (2000 rpm s^{-1} ; 30 s) directly on ITO.

The typical layer thickness was in the range of 30–50 nm as revealed from atomic force microscopy (AFM)-measurements. For AFM studies, a Multimode V scanner in conjunction with a Nanoscope V controller (Veeco Instruments) was used. Image processing and data analysis was performed using Gwyddion software version 2.40. Samples were measured in tapping mode using PPP-NCHR probes obtained from Nanoandmore in air.

Several scans were performed from different parts of the samples to check the uniformity of the surface. Final images were measured from a scanning area of $10 \times 10 \mu\text{m}^2$ with a tip velocity in the range from 16 to $18 \mu\text{m s}^{-1}$. No image processing except flattening was done. Roughness values were calculated as root-mean-square (rms) values.

All computations were performed using the Gaussian 09 package, revision A.02.²⁹ For the calculation of HOMO/LUMO levels of compounds **S1–3**, ground state (S_0) geometries were optimized in gas phase within C_3 symmetry using the Becke three parameters hybrid functional with Lee–Yang–Perdew correlation (B3LYP)^{30,31} in combination with Pople basis set 6-311+G*.³² To obtain vertical absorption and emission of model compounds **S_m1–3**, ground state S_0 and first excited singlet state S_1 were optimized applying DFT and time-dependent (TD) DFT level of theory using M06-2X^{33,34} functional in combination with the polarized double zeta SVP basis set.³⁵ This parameterization was shown to be superior in terms of accuracy for the calculation of vertical transitions.³⁶ Geometry optimizations were performed without symmetry constraints and solvent effects were included through the polarizable continuum model (PCM)³⁷ in its linear response (LR-PCM)³⁸ and state specific (SS-PCM)³⁹ formulations, always considering the equilibrium time regime (eq.) for the excited state.

General procedure for the synthesis of 6a–f

Synthesis was performed according to Goodbrand.²⁶ 4-Bromoaniline **4a** (1.0 eq.), substituted iodobenzene **5a–f** (2.2 eq.), KOH (7.8 eq.), CuCl (0.04 eq) and 1,10-phenanthroline monohydrate (0.04 eq.) were suspended in anhydrous toluene. After purging the apparatus with argon, the reaction mixture was refluxed on a Dean Stark trap for an appropriate time maintaining the argon atmosphere. Reaction progress was monitored by GC/MS. The reaction mixture was cooled to room temperature and water was added to solve the potassium hydroxide. Phases were separated and the hydrous phase was extracted with toluene three times. The combined organic layer was washed with brine, dried over anhydrous sodium sulfate and evaporated to dryness under reduced pressure. The obtained crude product was purified by Kugelrohr distillation and subsequent recrystallisation from methanol or acetonitrile.

4-Bromo-N,N-bis(4-fluorophenyl)benzeneamine (6c). According to the general procedure; **4a** (7.04 g, 41 mmol), **5c** (20.0 g, 90 mmol), KOH (17.94 g, 320 mmol), CuCl (162 mg, 1.6 mmol) and phenanthroline monohydrate (325 mg, 1.6 mmol) were refluxed for 16 h using 250 mL anhydrous toluene. Kugelrohr distillation ($130 \text{ }^\circ\text{C}$, 3.8×10^{-1} mbar) and recrystallization from methanol gave colourless crystals of **6c** (10.33 g, 70% of theory). TLC (silica gel, hexanes): $r_f = 0.36$. $F_p = 56\text{--}58 \text{ }^\circ\text{C}$. $^1\text{H NMR}$ (200 MHz, CD_2Cl_2): $\delta = 7.38\text{--}7.25$ (m, 2H), 7.11–6.91 (m, 4H), 6.89–6.72 (m, 8H), 6.91–6.80 (m, 2H) ppm. $^{13}\text{C NMR}$ (50 MHz, CD_2Cl_2): $\delta = 159.7$ (s, $J_{\text{CF}} = 242.6$ Hz), 147.8 (s), 144.0 (s, $J_{\text{CF}} = 2.8$ Hz), 132.7 (d), 126.9 (d, $J_{\text{CF}} = 8.1$ Hz), 124.3 (d), 116.7 (d, $J_{\text{CF}} = 22.6$ Hz), 114.7 (s) ppm. MS (EI): m/z 359 (M^+ , 100%), 279 (22), 184 (14).

4-Bromo-*N,N*-bis[4-(trimethylsilyl)phenyl]benzeneamine (6e). According to the general procedure; **4a** (7.82 g, 45.5 mmol), **5e** (27.62 g, 100 mmol), KOH (19.89 g, 355 mmol), CuCl (180 mg, 1.8 mmol) and phenanthroline monohydrate (360 mg, 1.8 mmol) were refluxed for 24 h using 250 mL anhydrous toluene. Kugelrohr distillation (130 °C, 6.5×10^{-2} mbar) and recrystallization from acetonitrile gave colourless crystals of **6e** (12.9 g, 60% of theory). TLC (silica gel, hexanes): $r_f = 0.39$. $F_p = 143\text{--}145$ °C. ^1H NMR (200 MHz, CDCl_3): $\delta = 7.42\text{--}7.27$ (m, 6H), 7.08–6.90 (m, 6H), 0.24 (s, 18H) ppm. ^{13}C NMR (100 MHz, CDCl_3): $\delta = 147.9$ (s), 146.9 (s), 134.64 (s), 134.61 (d), 132.4 (d), 126.1 (d), 123.5 (d), 115.5 (s), 112.4 (s), -0.8 (q) ppm. MS (EI): m/z 469 (M^+ , 100%), 454 (61), 452 (58), 220 (65).

4-Bromo-*N,N*-bis[4-(1,1-dimethylethyl)phenyl]benzeneamine (6f). According to the general procedure; **4a** (3.7 g, 21.5 mmol), **5f** (12.3 g, 47.3 mmol), KOH (9.4 g, 168 mmol), CuCl (85 mg, 0.86 mmol) and phenanthroline monohydrate (170 mg, 0.86 mmol) were refluxed for 36 h using 130 mL anhydrous toluene. Kugelrohr distillation (160 °C, 2.2×10^{-1} mbar) and recrystallization from acetonitrile gave colourless crystals of **6f** (5.8 g, 61% of theory). TLC (silica gel, hexanes): $r_f = 0.33$. $F_p = 165\text{--}168$ °C. ^1H NMR (200 MHz, CD_2Cl_2): $\delta = 7.36\text{--}7.22$ (m, 6H), 7.07–6.95 (m, 4H), 6.95–6.82 (m, 2H), 1.32 (s, 18H) ppm. ^{13}C NMR (50 MHz, CD_2Cl_2): $\delta = 148.1$ (s), 146.9 (s), 145.3 (s), 132.4 (d), 126.8 (d), 124.8 (d), 124.5 (d), 114.0 (s), 34.8 (s), 31.8 (q) ppm. MS (EI): m/z 435 (M^+ , 73%), 422 (96), 420 (100), 204 (35), 176 (47).

General procedure for the synthesis of **6g–6l** (nucleophilic substitution)

Synthesis was performed according to Davey⁴⁰ and Gorvin.^{40,41} Under an argon atmosphere, 4-haloaniline **4a,b** (1 eq.), fluoro-benzene **8a–c** (2.2 eq.) and base (CsF or KO^tBu , 2.0–2.2 eq.) were stirred in DMSO (stored over molecular sieve, 3 Å) at 120 °C overnight. The solvent was removed under reduced pressure and the remaining crude product dissolved in chloroform. After washing with water, the organic layer was dried over anhydrous sodium sulfate and evaporated to dryness under reduced pressure. Further purification was achieved by column chromatography or recrystallization.

4-Bromo-*N,N*-bis(4-nitrophenyl)benzeneamine (6g). Under an argon atmosphere, 4-bromoaniline (6.88 g, 40 mmol) and CsF (12.15 g, 80 mmol) were suspended in 100 mL of dry DMSO. To the stirred suspension **7a** (12.42 g, 88 mmol) was added drop wise and the reaction was heated to 110 °C for 40 h. After cooling to r.t., the reaction mixture was poured on 800 mL of water. The formed brown precipitate was filtered over a glass sinter funnel and crystallized from pyridine to give **6g** (9.00 g, 54% of theory) as yellow crystals. TLC (silica gel, hexanes/ethyl acetate = 9/1): $r_f = 0.76$. $F_p = 312\text{--}315$ °C. ^1H NMR (400 MHz, CDCl_3): $\delta = 8.19\text{--}8.10$ (m, 4H), 7.57–7.49 (m, 2H), 7.17–7.09 (m, 4H), 7.07–7.00 (m, 2H) ppm. ^{13}C NMR (100 MHz, CDCl_3): $\delta = 151.7$ (s), 144.2 (s), 143.3 (s), 133.9 (d), 128.7 (d), 125.9 (d), 122.8 (d), 120.5 (s) ppm. MS (EI): m/z 413 (M^+ , 100%), 323 (20), 321 (20), 241 (96).

4-Bromo-*N,N*-bis[4-(methylsulfonyl)phenyl]benzeneamine (6h). Under an argon atmosphere, 4-bromoaniline (86 mg, 0.5 mmol),

7b (192 mg, 1.1 mmol) and KO^tBu (118 mg, 1.05 eq.) were stirred in 2 mL of dry DMSO at 120 °C for 12 h. After cooling to r.t., the solvent was removed under reduced pressure. The residue was taken up with chloroform and filtered over a pad of celite. The solvent was removed under reduced pressure and the crude product purified by column chromatography (40 g silica gel, hexanes/ethyl acetate gradient 20 → 50%) to give **6h** as light brown powder (184 mg, 77% of theory). TLC (silica gel, hexanes/ethyl acetate = 1/1): $r_f = 0.20$. $F_p = 240$ °C. ^1H NMR (200 MHz, CDCl_3): $\delta = 7.86\text{--}7.73$ (m, 4H), 7.55–7.44 (m, 2H), 7.22–7.11 (m, 4H), 7.06–6.96 (m, 2H), 3.05 (s, 6H) ppm. ^{13}C NMR (50 MHz, CDCl_3): $\delta = 151.0$ (s), 144.5 (s), 134.8 (s), 133.6 (d), 129.4 (d), 128.4 (d), 123.2 (d), 119.7 (s), 44.8 (q) ppm.

4,4'-[[4-Bromophenyl]imino]bisbenzotrile (6i). Under an argon atmosphere, 4-bromoaniline (8.1 g, 47 mmol) and CsF (14.3 g, 94 mmol) were suspended in 120 mL of dry DMSO. A solution of **7c** (12.5 g, 103 mmol) in 50 mL of dry DMSO was added drop wise and the reaction mixture was heated to 110 °C for 50 h. After cooling to r.t., the reaction mixture was poured on 800 mL of water and extracted three times with 200 mL chloroform. The combined organic layer was washed with brine, dried over anhydrous sodium sulfate and the solvent was removed under reduced pressure. The crude product was crystallized from ethanol to give **6i** (4.05 g, 23% of theory) as light brown solid. TLC (silica gel, hexanes/ethyl acetate = 4/1): $r_f = 0.41$. $F_p = 261\text{--}262$ °C. ^1H NMR (200 MHz, CDCl_3): $\delta = 7.58\text{--}7.42$ (m, 6H), 7.14–7.03 (m, 4H), 7.03–6.93 (m, 2H) ppm. ^{13}C NMR (50 MHz, CDCl_3): $\delta = 149.9$ (s), 144.3 (s), 133.8 (d), 133.6 (d), 128.3 (d), 123.3 (d), 119.7 (s), 118.9 (s), 106.5 (s) ppm. MS (EI): m/z 373 (M^+ , 100%), 293 (29), 192 (38), 147 (80).

4-Iodo-*N,N*-bis(4-nitrophenyl)benzeneamine (6j). Under an argon atmosphere, 4-iodoaniline (5.6 g, 26 mmol) and KO^tBu (6.1 g, 54 mmol) were suspended in 150 mL of dry DMSO. To the stirred suspension **7a** (8.00 g, 57 mmol) was added drop wise and the reaction was heated to 120 °C for 40 h. After cooling to r.t., the solvent was removed under reduced pressure. The residue was taken up with chloroform and filtered over a pad of celite. The solvent was removed under reduced pressure and the crude product crystallized from pyridine to give **6j** (6.96 g, 58% of theory) as orange solid. TLC (silica gel, hexanes/ethyl acetate = 9/1): $r_f = 0.26$. $F_p = 295\text{--}297$ °C. ^1H NMR (400 MHz, CDCl_3): $\delta = 8.19\text{--}8.10$ (m, 4H), 7.76–7.68 (m, 2H), 7.17–7.09 (m, 4H), 6.94–6.87 (m, 2H) ppm. ^{13}C NMR (100 MHz, CDCl_3): $\delta = 151.6$ (s), 144.9 (s), 143.4 (s), 139.8 (d), 128.8 (d), 125.9 (d), 122.9 (d), 91.4 (s) ppm. MS (EI): m/z 461 (M^+ , 100%), 369 (11), 241 (83).

4-Iodo-*N,N*-bis[4-(methylsulfonyl)phenyl]benzeneamine (6k). Under an argon atmosphere, 4-iodoaniline (4.38 g, 20 mmol), **7b** (7.6 g, 44 mmol) and KO^tBu (4.94 g, 44 mmol) were stirred in 150 mL of dry DMSO at 120 °C for 18 h. After cooling to r.t., the solvent was removed under reduced pressure. The residue was taken up with 100 mL of chloroform and washed with 50 mL of water. After drying over anhydrous sodium sulfate, the solvent was removed under reduced pressure and the crude product was purified by recrystallization from acetic acid/water (v/v = 15/1) to give **6k** as a brown solid (6.74 g, 64% of theory).

TLC (silica gel, hexanes/ethyl acetate = 1/1): r_f = 0.19. F_p = 232–235 °C. ^1H NMR (200 MHz, CDCl_3): δ = 7.83–7.73 (m, 4H), 7.70–7.62 (m, 2H), 7.23–7.11 (m, 4H), 6.92–6.83 (m, 2H), 3.04 (s, 6H) ppm. ^{13}C NMR (50 MHz, CDCl_3): δ = 151.0 (s), 145.2 (s), 139.5 (d), 134.8 (s), 129.4 (d), 128.5 (d), 123.3 (d), 90.5 (s), 44.8 (q) ppm.

4,4'-[(4-Iodophenyl)imino]bisbenzotrile (6l). Under an argon atmosphere, 4-iodoaniline (4.48 g, 20.5 mmol) and CsF (6.52 g, 43 mmol) were suspended in 40 mL of dry DMSO. A solution of **7c** (5.45 g, 45 mmol) in 20 mL of dry DMSO was added drop wise and the reaction mixture was heated to 140 °C for 18 h. After cooling to r.t., the solvent was removed under reduced pressure. The residue was taken up with chloroform and filtered over a pad of celite. The solvent was removed under reduced pressure and the crude product purified by column chromatography (90 g silica gel, dry loading on 10 g silica, hexanes/ethyl acetate gradient 5 → 20%) to give **6l** (2.10 g, 24% of theory) as light yellow solid. TLC (silica gel, hexanes/ethyl acetate = 4/1): r_f = 0.42. F_p = 228–230 °C. ^1H NMR (200 MHz, CDCl_3): δ = 7.73–7.61 (m, 2H), 7.59–7.45 (m, 4H), 7.15–7.02 (m, 4H), 6.92–6.81 (m, 2H) ppm. ^{13}C NMR (50 MHz, CDCl_3): δ = 149.9 (s), 145.0 (s), 139.5 (d), 133.8 (d), 128.5 (d), 123.4 (d), 118.9 (s), 106.5 (s), 90.5 (s) ppm. MS (EI): m/z 421 (M^+ , 100%), 294 (12), 192 (12).

General procedure for the synthesis of 8a–f

Synthesis was performed according to Anemian:⁴² all operations were performed under argon atmosphere. Triphenylamine (**6a–f**) (1.0 eq.) was dissolved in anhydrous THF. The solution was cooled to –80 °C and a solution of *n*-butyllithium (2.5 M in hexanes) (1.2 eq.) was added *via* a syringe, keeping the temperature below –75 °C. The reaction mixture was stirred at –80 °C for appropriate time before isopropyl pinacol borate (1.2 eq.) was added drop-wise at the same temperature. After slowly warming to room temperature (approx. 2 h), stirring was continued overnight. The solvent was distilled off under reduced pressure and the residue was distributed between water and chloroform. The phases were separated and the aqueous phase was extracted twice with chloroform. The combined organic layer was washed with brine and dried over sodium sulfate. The solvent was removed under reduced pressure to give the crude product, which was further purified by recrystallization or Kugelrohr distillation.

***N,N*-Bis(4-fluorophenyl)-4-(4,4,5,5-tetramethyl-1,3,2-dioxaborolan-2-yl)benzeneamine (8c).** According to the general procedure; **6c** (4.8 g, 13.3 mmol) was lithiated with *n*-BuLi (6.4 mL, 16 mmol) in 50 mL anhydrous THF for 2 h before isopropyl pinacol borate (3.0 g, 16 mmol) was added. After general workup the crude product was purified by Kugelrohr distillation (130 °C, 8.0×10^{-2} mbar) to give **8c** as white crystalline powder (4.9 g, 91% of theory). TLC (silica gel, hexanes/ethyl acetate = 8/1): r_f = 0.67. F_p = 92–95 °C. ^1H NMR (200 MHz, CD_2Cl_2): δ = 7.65–7.53 (m, 2H), 7.16–6.84 (m, 10H), 1.31 (s, 12H) ppm. ^{13}C NMR (50 MHz, CD_2Cl_2): δ = 159.8 (s, J_{CF} = 242.8 Hz), 151.2 (s), 143.9 (s, J_{CF} = 3.2 Hz), 136.3 (d), 127.5 (d, J_{CF} = 8.2 Hz), 120.7 (d), 116.7 (d, J_{CF} = 22.6 Hz), 84.1 (s), 25.2 (q) ppm (C–B not detected). MS (EI): m/z 407 (M^+ , 100%), 349 (10), 307 (18).

***N,N*-Bis[4-(trimethylsilyl)phenyl]-4-(4,4,5,5-tetramethyl-1,3,2-dioxaborolan-2-yl)benzeneamine (8e).** According to the general

procedure; **6e** (7.03 g, 15 mmol) was lithiated with *n*-BuLi (7.2 mL, 18 mmol) in 75 mL of anhydrous THF for 2 h before isopropyl pinacol borate (3.35 g, 18 mmol) was added. After general workup the crude product was purified by recrystallization from acetonitrile to give **8e** as white crystalline powder (6.60 g, 85% of theory). TLC (silica gel, hexanes/ethyl acetate = 8/1): r_f = 0.72. F_p = 206–209 °C. ^1H NMR (200 MHz, CDCl_3): δ = 7.73–7.64 (m, 2H), 7.44–7.34 (m, 4H), 7.13–7.02 (m, 6H), 1.34 (s, 12H), 0.26 (s, 18H) ppm. ^{13}C NMR (50 MHz, CDCl_3): δ = 150.4 (s), 147.9 (s), 136.1 (d), 134.7 (s), 134.5 (d), 124.0 (d), 122.8 (d), 83.8 (s), 25.1 (q), –0.8 (q) ppm (C–B not detected). MS (EI): m/z 515 (M^+ , 100%), 500 (22), 400 (11), 243 (11).

***N,N*-Bis[4-(1,1-dimethylethyl)phenyl]-4-(4,4,5,5-tetramethyl-1,3,2-dioxaborolan-2-yl)benzeneamine (8f).** According to the general procedure; **6f** (10.91 g, 25 mmol) was lithiated with *n*-BuLi (12 mL, 30 mmol) in 150 mL of anhydrous THF for 2 h before isopropyl pinacol borate (5.58 g, 30 mmol) was added. After general workup the crude product was triturated with methanol to give **8f** as white crystalline powder (9.05 g, 79% of theory). TLC (silica gel, hexanes/ethyl acetate = 8/1): r_f = 0.71. F_p = 212–214 °C. ^1H NMR (200 MHz, CDCl_3): δ = 7.64–7.53 (m, 2H), 7.37–7.26 (m, 4H), 7.10–7.00 (m, 4H), 7.00–6.91 (m, 2H), 1.37–1.29 (m, 30H) ppm. ^{13}C NMR (50 MHz, CDCl_3): δ = 151.5 (s), 147.2 (s), 145.2 (s), 136.2 (d), 126.8 (d), 125.4 (d), 120.9 (d), 84.0 (s), 34.8 (s), 31.8 (q), 25.3 (q) ppm (C–B not detected). MS (EI): m/z 483 (M^+ , 16%), 468 (18), 368 (12), 168 (11), 57 (100).

***N,N*-Bis(4-nitrophenyl)-4-(4,4,5,5-tetramethyl-1,3,2-dioxaborolan-2-yl)benzeneamine (8g).** Synthesis was performed according to Murata.⁴³ In a 100 mL round-bottom flask, **6j** (2.08 g, 4.5 mmol, 1.0 eq.) and $\text{PdCl}_2(\text{dppf})$ (98.8 mg, 0.135 mmol, 0.03 eq.) were suspended in 20 mL of dry dioxane. After flushing the apparatus with argon, triethylamine (1.37 g, 13.5 mmol, 3.0 eq.) and pinacolborane (749 mg, 5.85 mmol, 1.3 eq.) were added drop wise. After stirring for 15 h at room temperature the solvent was removed under reduced pressure. The crude product was purified by column chromatography (100 g basic alumina, dry loading on 6 g neutral alumina, hexanes/DCM gradient 25 → 100%) to give **8g** as orange powder (390 mg, 19% of theory). TLC (silica gel, hexanes/ethyl acetate = 8/1): r_f = 0.52. F_p = 175–178 °C. ^1H NMR (200 MHz, CDCl_3): δ = 8.18–8.06 (m, 4H), 7.89–7.77 (m, 2H), 7.20–7.07 (m, 6H), 1.33 (s, 12H) ppm. ^{13}C NMR (50 MHz, CDCl_3): δ = 151.9 (s), 147.6 (s), 143.2 (s), 137.1 (d), 126.0 (d), 125.7 (d), 123.0 (d), 84.3 (s), 25.1 (q) ppm (C–B not detected). MS (EI): m/z 461 (M^+ , 100%), 361 (21), 268 (17).

General procedure for the Suzuki coupling towards 2, S1–3

The synthesis was performed according to Marion.⁴⁴ Under an argon atmosphere, (hetero)aromatic halide (1.0 eq.), boronic ester (3.0–4.5 eq.) and KO^tBu (3.0–4.5 eq.) were suspended in a sufficient amount of solvent (IPA/ H_2O = 3/1; degassed by bubbling with argon). A solution of (IPr)Pd(allyl)Cl (0.02–0.05 eq.) in degassed IPA was added and the reaction mixture was refluxed for an appropriate time, monitoring the conversion by TLC. After completion, the reaction mixture was distributed between water and chloroform; the phases were separated and the aqueous

layer was extracted with chloroform three times. The combined organic layer was dried over anhydrous sodium sulfate and the solvent removed under reduced pressure to give the crude product. Purification was achieved by column chromatography.

2,2',2''-(1,3,5-Benzenetriyl)tristhiophene (2). According to the general procedure; 1,3,5-tribromobenzene (0.787 g, 2.5 mmol), 2-thiopheneboronic acid pinacol ester (2.364 g, 11.25 mmol) and KO^tBu (1.262 g, 11.25 mmol) were suspended in 50 mL solvent. (IPr)Pd(allyl)Cl (71.4 mg, 125 μmol; dissolved in 1 mL IPA) was added before refluxing for 1 h. After general workup the crude product was purified by column chromatography (90 g silica gel, hexanes/DCM 0 → 3%) to give **2** as white powder (0.697 g, 86% of theory). TLC (silica gel, hexanes/ethyl acetate = 20/1): r_f = 0.35. ¹H NMR (200 MHz, CDCl₃): δ = 7.74 (s, 3H), 7.40 (dd, J = 1.1, 3.6 Hz, 3H), 7.33 (dd, J = 1.1, 5.1 Hz, 3H), 7.11 (dd, J = 3.6, 5.1 Hz, 3H) ppm. ¹³C-NMR (50 MHz, CDCl₃): δ = 143.7 (s), 135.9 (s), 128.3 (d), 125.6 (d), 124.1 (d), 122.9 (d) ppm.

4,4',4''-(1,3,5-Benzenetriyltri-5,2-thiophenediyl)tris[*N,N*-diphenylbenzenamine] (S1). According to the general Suzuki procedure; compound **3** (280.1 mg, 0.5 mmol), boronic acid pinacol ester **6a** (835.0 mg, 2.25 mmol) and KO^tBu (252.5 mg, 2.25 mmol) were suspended in 12 mL solvent. (IPr)Pd(allyl)Cl (14.3 mg, 25 μmol; dissolved in 1 mL IPA) was added before refluxing for 2 h. After general workup the crude product was purified by column chromatography (90 g silica gel, hexanes/DCM = 6/1); after removing the solvent under reduced pressure, the residue was dissolved in 40 mL of boiling 2-butanone. The product was precipitated by adding 50 mL of 2-propanol to give **S1** as yellow powder (512.8 mg, 97% of theory). TLC (silica gel, cyclohexane/DCM = 3/1): r_f = 0.30. ¹H NMR and ¹³C NMR data according to literature.²¹ MS (MALDI-TOF): calcd for C₇₂H₅₁N₃S₃: 1053.3245; found: 1053.3020.

4,4',4''-(1,3,5-Benzenetriyltri-5,2-thiophenediyl)tris[*N,N*-bis-(4-methylphenyl)benzenamine] (S2). According to the general Suzuki procedure; compound **3** (280.1 mg, 0.5 mmol), boronic acid pinacol ester **6b** (898.5 mg, 2.25 mmol) and KO^tBu (252.5 mg, 2.25 mmol) were suspended in 12 mL solvent. (IPr)Pd(allyl)Cl (14.3 mg, 25 μmol; dissolved in 1 mL IPA) was added before refluxing for 2 h. After general workup the crude product was purified by column chromatography (90 g silica gel, hexanes/DCM 25 → 27%) to give **S2** as yellow powder (473.3 mg, 83% of theory). TLC (silica gel, cyclohexane/DCM = 3/1): r_f = 0.30. ¹H NMR (200 MHz, CD₂Cl₂): δ = 7.74 (s, 3H), 7.53–7.44 (m, 6H), 7.40 (d, J = 3.78 Hz, 3H), 7.23 (d, J = 3.80 Hz, 3H), 7.15–7.05 (m, 12H), 7.05–6.94 (m, 18H), 2.32 (s, 18H) ppm. ¹³C NMR (50 MHz, CD₂Cl₂): δ = 148.5 (s), 145.5 (s), 144.9 (s), 141.8 (s), 136.2 (s), 133.7 (s), 130.50 (d), 127.5 (s), 126.8 (d), 125.45 (d), 125.39 (d), 123.4 (d), 122.6 (d), 121.7 (d), 20.1 (s) ppm. MS (MALDI-TOF): calcd for C₇₈H₆₃N₃S₃: 1137.4184; found: 1137.4006.

4,4',4''-(1,3,5-Benzenetriyltri-5,2-thiophenediyl)tris[*N,N*-bis-(4-fluorophenyl)benzenamine] (S3). According to the general procedure; compound **3** (280.6 mg, 0.5 mmol), boronic acid pinacol ester **6c** (916.3 mg, 2.25 mmol) and KO^tBu (252.5 mg, 2.25 mmol) were suspended in 12 mL solvent. (IPr)Pd(allyl)Cl (14.3 mg, 25 μmol; dissolved in 1 mL IPA) was added before refluxing for 2 h. After general workup the crude product was

purified by column chromatography (90 g silica gel, hexanes/DCM 25 → 30%) to give **S3** as yellow powder (323.3 mg, 56% of theory). TLC (silica gel, hexanes/DCM = 5/1): r_f = 0.32. ¹H NMR (200 MHz, CD₂Cl₂): δ = 7.72 (s, 3H), 7.56–7.45 (m, 6H), 7.39 (d, J = 3.76 Hz, 3H), 7.24 (d, J = 3.78 Hz, 3H), 7.14–6.92 (m, 30H) ppm. ¹³C NMR (50 MHz, CD₂Cl₂): δ = 159.7 (s, J_{CF} = 242.5 Hz), 148.2 (s), 144.6 (s), 144.1 (s, J_{CF} = 3.0 Hz), 142.1 (s), 136.1 (s), 128.2 (s), 126.98 (d), 126.97 (d, J_{CF} = 8.1 Hz), 125.4 (d), 123.7 (d), 122.8 (d), 121.8 (d), 116.7 (d, J_{CF} = 22.7 Hz) ppm. MS (MALDI-TOF): calcd for C₇₂H₄₅F₆N₃S₃: 1161.2680; found: 1161.3152.

Results and discussion

Synthesis

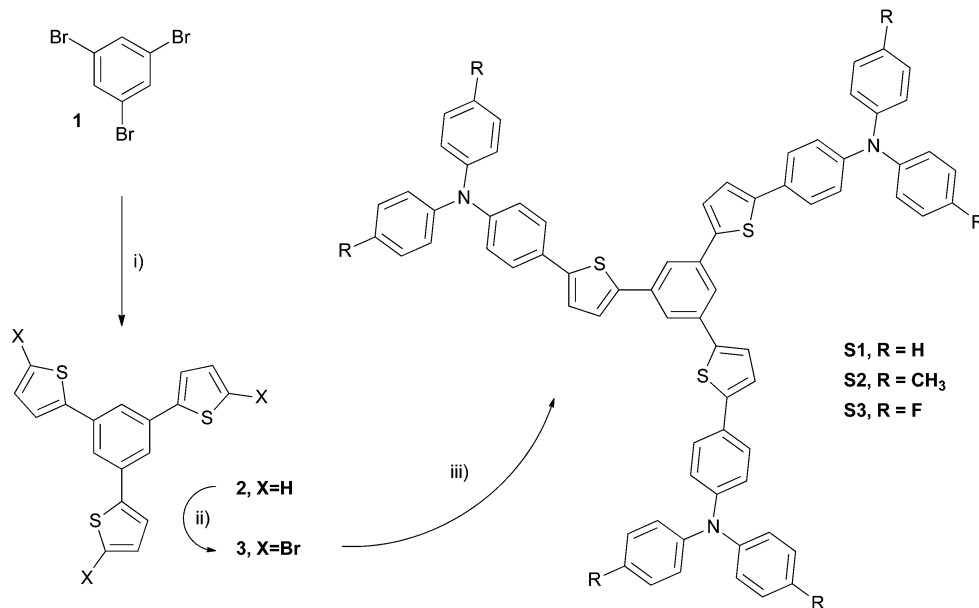
The synthetic linkage of TPA structures **8** bearing either electron withdrawing (–I, –M-effect) or donating (+I, +M) substituents with **3** is realized *via* Suzuki cross-coupling reactions.^{45,46} Therefore, a general cross-coupling procedure was developed tolerating a broad spectrum of functionalized TPA boronic acid esters (Scheme 1).

Stille cross-coupling reactions are commonly applied in literature,⁴⁷ however they require toxic stannyl intermediates. In order to avoid these undesirable precursors, highly stable pinacol boronic acid esters are used in Suzuki cross-coupling reactions ensuring high conversion, selectivity, and tolerance of functional groups representing a more convenient synthetic approach.⁴⁸ Herein we report the synthetic pathway towards diversely substituted triphenylamine structures (R = –H, –Me, –OMe, –TMS, –*t*Bu, –F, –NO₂, –CN, –SO₂Me), functionalization towards boronic acid esters and subsequent cross-coupling with brominated tris(2-thienyl)benzene **3** *via* Suzuki reaction.

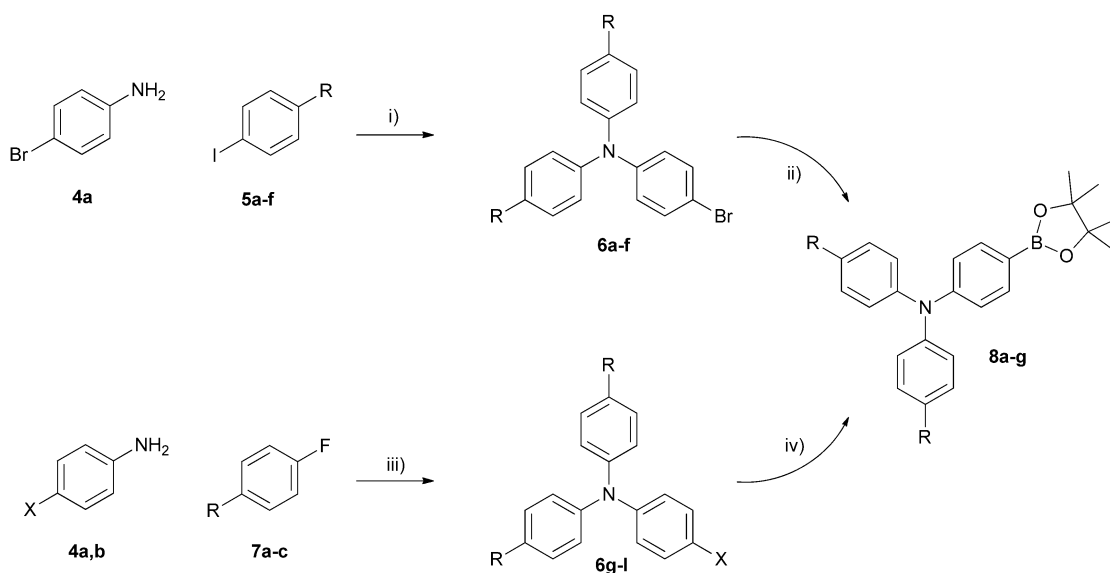
In order to synthesize the desired TPA building blocks two synthetic pathways towards halide species **6a–I** were developed depending on the nature of substituent R (Scheme 2).

The conversion of suitably substituted iodobenzenes **5a–f** and 4-bromoaniline **4a** to the corresponding bromo substituted triphenylamines **6a–f** was realized in good to excellent yields *via* Ullmann condensation applying copper(i)chloride and 1,10-phenanthroline as catalytic system.²⁶ When applying the same strategy on substrates bearing –M substituents relatively low conversions have been observed. Consequently, nucleophilic aromatic substitution of properly substituted fluorobenzenes **7a–c** with anilines **4a,b** was chosen as an alternative synthetic approach leading to bromo (**6g–i**) and iodo (**6j–l**) substituted triphenylamine derivatives in good yields (Table 1).

The synthesis of the boronic acid pinacolates **8a–f** was achieved *via* metal halogen exchange using *n*-butyllithium and further conversion with isopropyl pinacol borate in good yields (Table 1). Again, substrates bearing –M substituent turned out to be troublesome, since neither bromo **6g–i** nor iodo derivatives **6k,l** showed proper conversion. Nevertheless, starting from iodo derivative **6j** the synthesis of boronic acid esters **8g** could be achieved (despite the rather low yields of 18%) when switching to the palladium catalyzed Miyaura borylation using pinacol borane as boron source (Scheme 2).



Scheme 1 Synthetic pathway towards **S1–3**. Reaction conditions: (i) thiophene-2-boronic acid pinacol ester, KO^tBu , $(\text{IPr})\text{Pd}(\text{allyl})\text{Cl}$, isopropanol/water, reflux; (ii) NBS, chloroform/glacial acetic acid, r.t.; (iii) **8a–c**, KO^tBu , $(\text{IPr})\text{Pd}(\text{allyl})\text{Cl}$, isopropanol/water, reflux.



Scheme 2 Synthesis of intermediates **6** and boronic acid esters **8**. Reaction conditions: (i) KOH , CuCl , phenanthroline in toluene, reflux; (ii) $n\text{-BuLi}$, $-78\text{ }^\circ\text{C}$ in THF, then isopropyl pinacol borate; (iii) CsF or KO^tBu in DMSO, ΔT ; (iv) pinacolborane, triethylamine, $\text{PdCl}_2(\text{dppf})$ in dioxane, r.t. For a definition of R and X please refer to Table 1.

Table 1 Experimental data for compounds **6a–l** and boronic acid esters **8a–f**

Ullmann condensation		Nucleophilic aromatic substitution		Synthesis of boronic esters					
R	Yield (%)	X	R	Yield (%)	R	Yield (%)			
6a	H	74	6g	Br	NO_2	54	8a	H	77
6b	Me	89	6h	Br	SO_2Me	77	8b	Me	74
6c	F	70	6i	Br	CN	23	8c	F	91
6d	OMe	86	6j	I	NO_2	58	8d	OMe	76
6e	TMS	60	6k	I	SO_2Me	64	8e	TMS	85
6f	<i>t</i> Bu	61	6l	I	CN	24	8f	<i>t</i> Bu	79

For the consecutive Suzuki cross-coupling reaction, palladium NHC-complex $(\text{IPr})\text{Pd}(\text{allyl})\text{Cl}$ showed superior efficiency over tetrakis(triphenyl)palladium(0) in terms of reactivity and selectivity. Additionally, high conversion and high tolerance of TPA boronic acid esters **8a–f** bearing either electron donating (e.g. $-\text{Me}$) or electron withdrawing substituents (e.g. $-\text{F}$) were observed using isopropanol–water as solvent and K^tOBu as base.

Applying these reaction conditions, compounds **2** and **S1–3** were obtained. The synthesis of **2** was achieved in good yield of 86% *via* cross-coupling of thiophene-2-boronic acid pinacol

Table 2 Photophysical characterization of compounds **S1–3** and computational data for compounds **S_m1–3**

Comp.	λ_{\max} (ϵ_{\max}) ^a (nm)	λ_{\max} ^b (nm)	λ_{em} (ϕ_f) ^c (nm)	λ_{em} ^d (nm)	λ_{em} ^e (nm)	Comp.	λ_{\max} ^f (nm)	λ_{em} ^g (nm)	λ_{em} ^h (nm)
S1	302 (61.2), 387 (112.9)	474	461 (62)	471	486	S_m1	344	450	445
S2	304 (61.7), 394 (104.2)	482	474 (71)	477	498	S_m2	349	454	459
S3	297 (51.0), 384 (104.7)	472	459 (62)	466	482	S_m3	343	449	445

^a Measured in THF solution, $\epsilon_{\max} \times 10^{-3}$ in $\text{M}^{-1} \text{cm}^{-1}$ in parentheses. ^b Absorption of solid samples. ^c Measured in a THF solution; ϕ_f fluorescence quantum yield. ^d Film samples. ^e Solid samples. ^f Calculated absorption of model compounds **S_m1–3**. ^g Calculated emission (LR-PCM) of model compounds **S_m1–3**. ^h Calculated emission (SS-PCM) of model compounds **S_m1–3**.

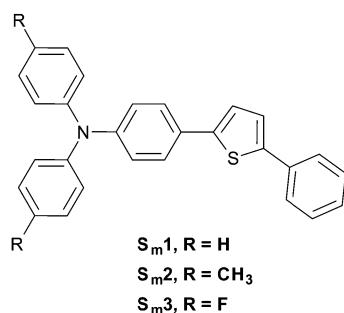
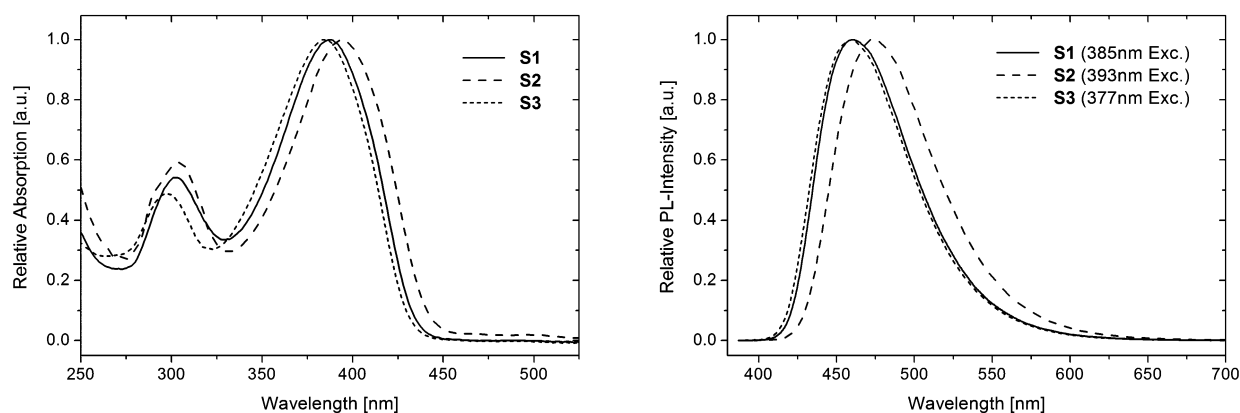
ester and 1,3,5-tribromobenzene **1** according to the above protocol. Consecutive bromination with NBS in chloroform/glacial acetic acid gave the tribromo derivative **3**, the precursor for the final Suzuki coupling with boronic acid esters **8a–c**. Star-shaped compounds **S1–3** bearing either electron donating or withdrawing substituents were obtained in satisfactory to excellent yields (Table 3). These solid materials appear yellow in color and are soluble in common organic solvents. The characterization of **S1–3** was performed by $^1\text{H}/^{13}\text{C}$ -NMR spectroscopy and HR-MS analysis. The data are consistent with the proposed structural formulations.

Photo-physical properties of **S1–3** were determined by UV-VIS and fluorescence spectrometry in THF solution, for amorphous films and in the solid state (Table 2 and Fig. 3). Two absorption maxima were located in relatively narrow ranges of 297–304 and 384–394 nm for substances **S1–3** when measured in THF solution. While the former is assigned to the

$n-\pi^*$ transition of the triphenylamine moiety, the longer wavelength absorption originates from the $\pi-\pi^*$ transitions of the electron-donating triphenylamine moiety to the electron-accepting thiophene moiety.⁴⁹ A clear trend can be observed, as the electron withdrawing fluoro derivative **S3** shows the absorption maximum with the highest energy, whereas the electron donating methyl derivative **S2** has the absorption maximum at the longest wavelength; the absorption maximum of the electron neutral **S1** lies in between.

These findings are supported by quantum chemical calculations of model substances **S_m1–3** (Fig. 2). In order to mimic C_3 symmetric substances **S1–3**, suitable model substances were chosen, comprising one dendritic arm and the benzene core. This approach ensures a realistic representation of **S1–3** while keeping the computational costs at a reasonable level. Absorption and emission wavelengths in THF of **S_m1–3** were estimated by applying density functional (DFT) and time dependent density functional (TDDFT) level of theory according to a protocol presented recently.³⁶ The calculated absorption and emission wavelengths of **S_m1–3** are in agreement with experimental data of **S1–3** showing the lowest shift in emission for fluoro-substituted **S3/S_m3** and highest emission shifts for methyl-substituted compounds **S2/S_m2** (Table 2).

Again this behavior can be correlated to the increased electron density on the aromatic ring (Fig. 3) in the case of **S2** ($\lambda_{\text{em}} = 474 \text{ nm}$) causing a significant bathochromic shift and a decreased electron density in the case of **S3** ($\lambda_{\text{em}} = 459 \text{ nm}$) causing a hypsochromic shift in reference to **S1** ($\lambda_{\text{em}} = 461 \text{ nm}$) (Table 2). Stokes shifts for all compounds **S1–3** are comparable and range from 0.51–0.53 eV. Quantum yields in solution are

Fig. 2 Model substances **S_m1–3**.Fig. 3 Absorption (left) and emission (right) spectra of **S1–3** in THF solution.

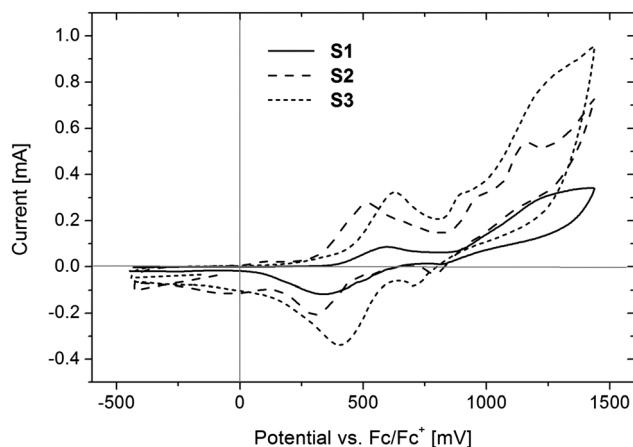


Fig. 4 Cyclic voltammograms of **S1–3** in DCM.

shifted to higher values correlating with enhanced electron density (Table 2). The values of **S1** and **S3** are identical ($\phi_f = 0.62$), whereas

Table 3 Experimental data, physical characterization and computational data of compounds **S1–3**

Comp.	Yield (%)	T_g^a (°C)	T_d^b (°C)	Band gap ^c (nm, eV)	HOMO/LUMO ^d (eV)	HOMO/LUMO ^e (eV)
S1	97	128	541	387, 3.20	−5.19/−1.99	−5.17/−1.76
S2	83	135	528	394, 3.14	−5.24/−2.10	−5.01/−1.66
S3	50	121	538	384, 3.23	−5.21/−1.98	−5.36/−1.91

^a Obtained from DSC measurements. ^b Thermal decomposition temperature determined from 5% mass loss. ^c Bandgaps were determined from the onsets of the absorption in THF solution. ^d HOMO-levels determined from solutions measured in DCM. All E_{ox} data are reported relative to ferrocene (Fc/Fc^+ , $E_{ox} = 446$ mV). The concentration of the compounds used in this experiment was $1 \text{ mg } \mu\text{L}^{-1}$ and the scan rate was 50 mV s^{-1} . LUMO levels were determined from the optical band gap and the HOMO energy level according to the following equation: $E_{LUMO} = E_{HOMO} + E_{bandgap}$. ^e Calculated HOMO/LUMO levels (B3LYP/6-311+G(d)).

the quantum yield is considerably higher ($\phi_f = 0.71$) for the methyl substituted derivative **S2**.

Emission spectra of solid samples **S1–3** are in the narrow range of 482–498 nm, whereas spin coated samples are in the range of 466–477 nm (for spectra please refer to the ESI†).

Electro-chemical characteristics of the star-shaped molecules **S1–3** were investigated by cyclic voltammetric methods (Fig. 4). The first oxidation potentials were used to determine the HOMO energy levels. Ferrocene served as an external standard for calibrating the potential and calculating the HOMO levels (−4.8 eV). All compounds **S1–3** undergo reversible oxidation indicating the formation of stable cation radicals. Only small variations of HOMO levels (−5.19 eV to −5.24 eV) were observed. The LUMO levels were determined from the optical bandgap and the HOMO energy level obtained from CV measurements and vary in the range from −1.98 to −2.10 eV. Calculated HOMO/LUMO levels are in good accordance with the experimental data for compounds **S1** and **S3**, whereas the deviation is somewhat higher for substance **S2**. The pertinent data are listed in Table 3.

Thermal properties were investigated by DSC and TGA measurements. Glass-forming properties and thermal stability of the compounds were examined by simultaneous thermal analysis (STA). The glass transition temperature (T_g) was estimated from DSC curves (Fig. 5). The determined T_g values are in the range from 121 to 135 °C, the methyl substituted **S2** showing the highest value while fluoro substituted **S3** exhibits the lowest T_g . All materials exhibit high thermal stability as evidenced by decomposition temperatures corresponding to 5% mass loss between 528 and 541 °C (Table 3 and Fig. 5). This high thermal stability allows for fabrication of homogeneous and stable amorphous thin films by vacuum deposition.

The semiconducting properties of the materials under investigation were tested by using a top-contact OFET architecture as shown in Fig. 6. A hole mobility up to $7.7 \times 10^{-4} \text{ cm}^2 \text{ V}^{-1} \text{ s}^{-1}$

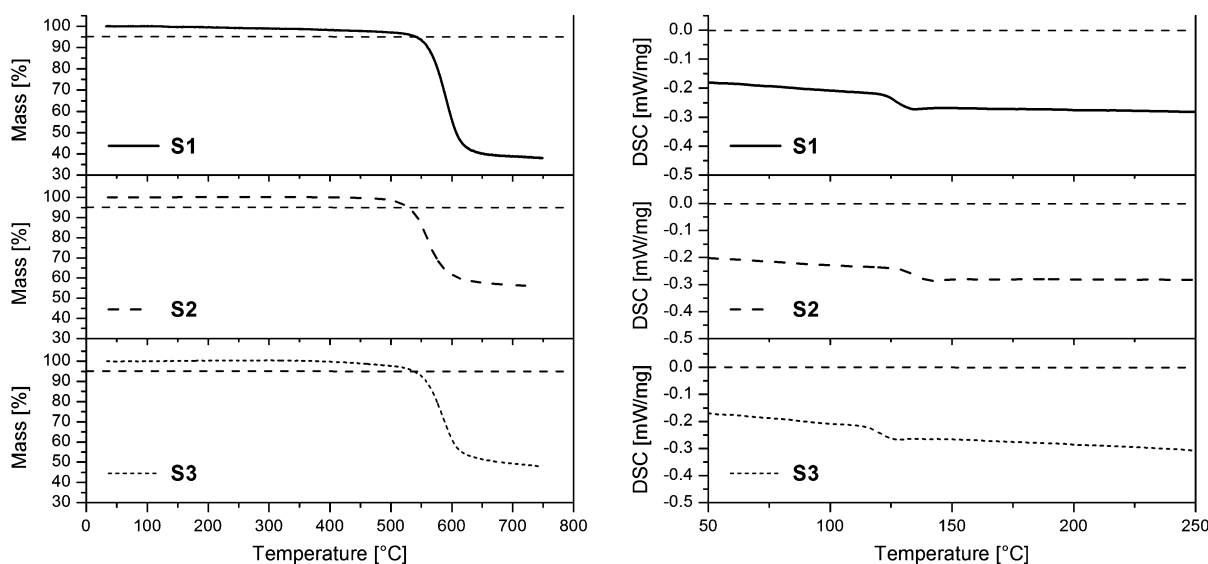


Fig. 5 TGA (left) and DSC (right) measurements of **S1–3**.

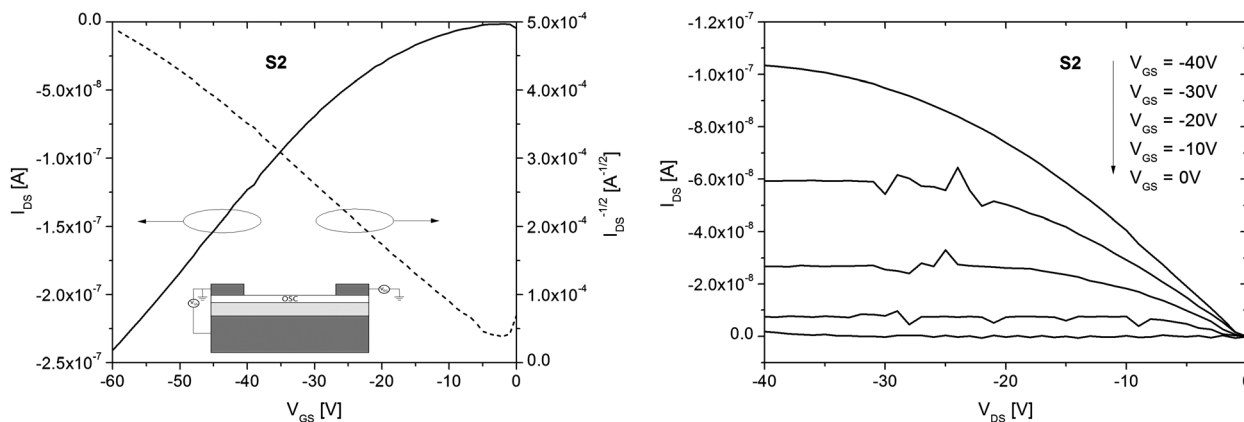


Fig. 6 Output characteristics (left) and corresponding transfer curve (right) of **S2**.

and average threshold voltages of approx. 0 V which can be attributed to a low background charge density in the material were recorded using **S2** as semiconducting layer (Fig. 6), while no working OFET device could be fabricated using **S1** or **S3**. As the performance of an OFET highly depends on the quality of the interface between dielectric and organic semiconductor, these results might be correlated to the tendency of **S2** to form nearly defect free films, which was observed in spin coating experiments.

All compounds **S1–3** readily form stable glasses. Spin coated thin films of **S1–3** were produced on ITO substrates using chloroform as solvent. Their surface morphology and thickness were further investigated by atomic force microscopy (AFM, Fig. 7). In principle, all films showed very little average

thickness (30–50 nm) and low roughness of the surface (root mean square = 0.63, 0.32 and 0.34 nm for **S1**, **S2** and **S3** respectively). However, when examining the surface of **S1** sub- μm sized pinholes were observed. Potential reasons for pinholes are trapped air, solvent gas-bubble formation or contaminations on the substrate or in the organic solution. Since numerous spin coating samples were prepared applying the same procedure yielding reproducible results, the origin of these defects is unlikely to come from the fabrication process. Therefore, the formation of these pinholes is probably substance specific and might be attributed to higher propensity to crystallization of **S1** compared to **S2** and **S3**. Thus, in contrast to **S1**, solution-processed films of **S2** and **S3** can readily be prepared.

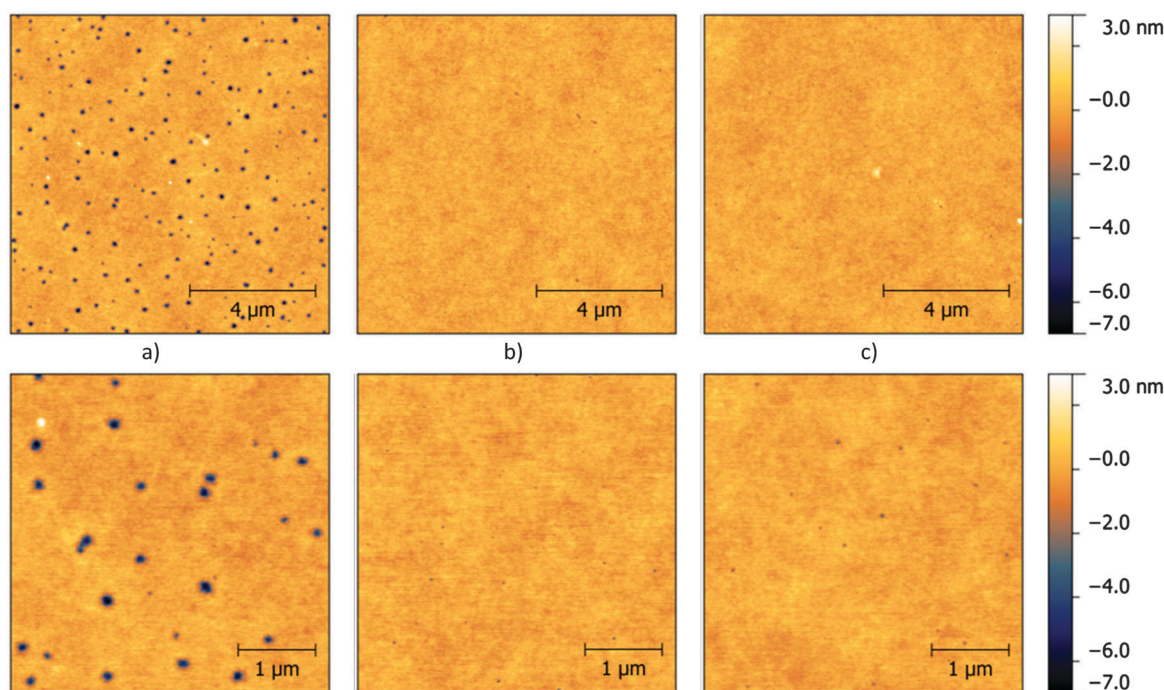


Fig. 7 Topography AFM images of **S1–3** (a–c).

Conclusion

This contribution outlines an optimized synthetic pathway towards a broad spectrum of *p*-substituted triphenylamines, suitable as building blocks for organic semiconducting materials.

We employed these triphenylamine moieties in C_3 symmetric dendritic tris(2-thienyl)benzene structures and elucidated the influence of the molecular design on photo-physical properties. The electronic characteristics of the substituents show a strong influence on the fluorescence spectra thus enabling color tuning. These star shaped materials exhibit good solubility and thermal stability allowing for both solution processing and physical vapor deposition, respectively. The novel materials were tested as semiconductors in organic field effect transistor devices, exhibiting hole mobilities of almost $10^{-3} \text{ cm}^2 \text{ V}^{-1} \text{ s}^{-1}$.

Spin coating experiments showed a strong correlation between the nature of the substituents and the morphology of the resulting thin film; similar results were observed for transistor performance. The structural versatility and capability of our molecular design will contribute to the further development of functional organic materials.

Acknowledgements

J. Binteringer gratefully acknowledges funding from the Marshall Plan Foundation. The authors thank Dr K. Föttinger for supporting the photophysical characterization, D. Bomze, A. Aster, M. Lunzer and K. Kandra for contributing to the synthetic experiments. M. Eberl is acknowledged for assisting in cyclic voltammetric measurements and K. Fohringer and P. Kautny for STA measurements.

References

- 1 S. R. Forrest, *Nature*, 2004, **428**, 911.
- 2 J. Mei, Y. Diao, A. L. Appleton, L. Fang and Z. Bao, *J. Am. Chem. Soc.*, 2013, **135**, 6724.
- 3 Y.-S. Tyan, *J. Photonics Energy*, 2011, **1**, 011009.
- 4 M. C. Scharber and N. S. Sariciftci, *Prog. Polym. Sci.*, 2013, **38**, 1929.
- 5 B. Kippelen and J.-L. Brédas, *Energy Environ. Sci.*, 2009, **2**, 251.
- 6 H. Klauk, *Organic electronics II: more materials and applications*, Wiley-VCH, Weinheim, 2012.
- 7 Y. Yamashita, *Sci. Technol. Adv. Mater.*, 2009, **10**, 024313.
- 8 Y. Shirota and H. Kageyama, *Chem. Rev.*, 2007, **107**, 953.
- 9 J. Kwon, M. K. Kim, J.-P. Hong, W. Lee, S. Lee and J.-I. Hong, *Bull. Korean Chem. Soc.*, 2013, **34**, 1355.
- 10 F. Geiger, M. Stoldt, H. Schweizer, P. Bäuerle and E. Umbach, *Adv. Mater.*, 1993, **5**, 922.
- 11 S. H. Kim, K. Hong, K. H. Lee and C. D. Frisbie, *ACS Appl. Mater. Interfaces*, 2013, **5**, 6580.
- 12 Y. Shirota, *J. Mater. Chem.*, 2000, **10**, 1.
- 13 N. Metri, X. Sallenave, C. Plesse, L. Beouch, P.-H. Aubert, F. Goubard, C. Chevrot and G. Sini, *J. Phys. Chem. C*, 2012, **116**, 3765.
- 14 J. Zhang, D. Deng, C. He, Y. He, M. Zhang, Z.-G. Zhang, Z. Zhang and Y. Li, *Chem. Mater.*, 2011, **23**, 817.
- 15 Z. Ning and H. Tian, *Chem. Commun.*, 2009, 5483.
- 16 A. Iwan, D. Sek, D. Pocięcha, A. Sikora, M. Palewicz and H. Janeczek, *J. Mol. Struct.*, 2010, **981**, 120.
- 17 A. Iwan and D. Sek, *Prog. Polym. Sci.*, 2011, **36**, 1277.
- 18 T. Noda, H. Ogawa, N. Noma and Y. Shirota, *Adv. Mater.*, 1997, **9**, 720.
- 19 J. Roncali, P. Leriche and A. Cravino, *Adv. Mater.*, 2007, **19**, 2045.
- 20 C. He, Q. He, Y. Yi, G. Wu, F. Bai, Z. Shuai and Y. Li, *J. Mater. Chem.*, 2008, **18**, 4085.
- 21 A. Cravino, S. Roquet, P. Leriche, O. Alévêque, P. Frère and J. Roncali, *Chem. Commun.*, 2006, 1416.
- 22 T.-T. Bui, L. Beouch, X. Sallenave and F. Goubard, *Tetrahedron Lett.*, 2013, **54**, 4277.
- 23 N. Metri, X. Sallenave, L. Beouch, C. Plesse, F. Goubard and C. Chevrot, *Tetrahedron Lett.*, 2010, **51**, 6673.
- 24 K. R. Justin Thomas, J. T. Lin, Y.-T. Tao and C.-W. Ko, *Chem. Mater.*, 2002, **14**, 1354.
- 25 A. Iwan, H. Janeczek, B. Kaczmarczyk, B. Jarzabek, M. Sobota and P. Rannou, *Spectrochim. Acta, Part A*, 2010, **75**, 891.
- 26 H. B. Goodbrand and N.-X. Hu, *J. Org. Chem.*, 1999, **64**, 670.
- 27 M. W. Andersen, B. Hildebrandt, G. Köster and R. W. Hoffmann, *Chem. Ber.*, 1989, **122**, 1777.
- 28 O. Navarro and S. P. Nolan, *Synthesis*, 2006, 366.
- 29 J. Frisch, G. W. Trucks, H. B. Schlegel, G. E. Scuseria, M. A. Robb, J. R. Cheeseman, G. Scalmani, V. Barone, B. Mennucci, G. A. Petersson, H. Nakatsuji, M. Caricato, X. Li, H. P. Hratchian, A. F. Izmaylov, J. Bloino, G. Zheng, J. L. Sonnenberg, M. Hada, M. Ehara, K. Toyota, R. Fukuda, J. Hasegawa, M. Ishida, T. Nakajima and Y. Honda, *Gaussian 09, Revision A.02*, Gaussian, Inc., Wallingford, CT, 2009.
- 30 C. Lee, W. Yang and R. G. Parr, *Phys. Rev. B: Condens. Matter Mater. Phys.*, 1988, **37**, 785.
- 31 A. D. Becke, *J. Chem. Phys.*, 1993, **98**, 5648.
- 32 R. Krishnan, J. S. Binkley, R. Seeger and J. A. Pople, *J. Chem. Phys.*, 1980, **72**, 650.
- 33 Y. Zhao and D. G. Truhlar, *Theor. Chem. Acc.*, 2007, **120**, 215.
- 34 Y. Zhao and D. G. Truhlar, *Theor. Chem. Acc.*, 2008, **119**, 525.
- 35 A. Schäfer, H. Horn and R. Ahlrichs, *J. Chem. Phys.*, 1992, **97**, 2571.
- 36 D. Lumpi, E. Horkel, F. Plasser, H. Lischka and J. Fröhlich, *ChemPhysChem*, 2013, **14**, 1016.
- 37 M. Cossi, V. Barone, R. Cammi and J. Tomasi, *Chem. Phys. Lett.*, 1996, **255**, 327.
- 38 M. Cossi and V. Barone, *J. Chem. Phys.*, 2001, **115**, 4708.
- 39 R. Improta, G. Scalmani, M. J. Frisch and V. Barone, *J. Chem. Phys.*, 2007, **127**, 074504.
- 40 M. H. Davey, V. Y. Lee, L.-M. Wu, C. R. Moylan, W. Volksen, A. Knoesen, R. D. Miller and T. J. Marks, *Chem. Mater.*, 2000, **12**, 1679.
- 41 J. H. Gorvin, *J. Chem. Soc., Perkin Trans. 1*, 1988, 1331.

- 42 R. Anemian, D. C. Cupertino, P. R. Mackie and S. G. Yeates, *Tetrahedron Lett.*, 2005, **46**, 6717.
- 43 M. Murata, T. Oyama, S. Watanabe and Y. Masuda, *J. Org. Chem.*, 2000, **65**, 164.
- 44 N. Marion, O. Navarro, J. Mei, E. D. Stevens, N. M. Scott and S. P. Nolan, *J. Am. Chem. Soc.*, 2006, **128**, 4101.
- 45 A. Leliège, J. Grolleau, M. Allain, P. Blanchard, D. Demeter, T. Rousseau and J. Roncali, *Chem. – Eur. J.*, 2013, **19**, 9948.
- 46 J. K. Choi, K. Cho and T.-H. Yoon, *Synth. Met.*, 2010, **160**, 1938.
- 47 R. A. Rossi, *J. Organomet. Chem.*, 2014, **751**, 201.
- 48 R. Martin and S. L. Buchwald, *Acc. Chem. Res.*, 2008, **41**, 1461.
- 49 Z. Ge, T. Hayakawa, S. Ando, M. Ueda, T. Akiike, H. Miyamoto, T. Kajita and M. Kakimoto, *Adv. Funct. Mater.*, 2008, **18**, 584.